



Novel Insulation Material Based on Basalt Fibres and Silica Aerogels

Thilo Becker^{a,*}, Davide Pico^b, Julia Lipin^a, Terence Lehmann^a, Alexander Lüking^a, Michael Hitz^c, Thomas Gries^a

^aInstitut für Textiltechnik der RWTH Aachen University, Otto-Blumenthal-Strasse 1, 52074 Aachen, Germany

^bISOLITE GmbH, Industriestraße 125, 67063 Ludwigshafen am Rhein, Germany

^cGETA mbH, Im Unteren Feld 10, 88239 Wangen im Allgäu, Germany

thilo.becker@ita.rwth-aachen.de

Basalt fibre reinforced silica aerogel composites with two different fibre lengths and two different fibre volume contents were successfully produced and analysed. After aging and drying of the fibre reinforced aerogel specimens, the geometrical data as well as the weight of each specimen were registered. The microstructure of selected specimens was recorded by tomography. Three-point bending tests were carried out in order to evaluate the effects of the fibrous reinforcement. The shrinkage of the samples was reduced with increasing fibre volume fractions. Specimen with a fibre length of 3.2 mm and a fibre volume fraction of 1.5 % showed the most homogeneous fibre distribution. Specimens with a fibre length of 12.7 mm fibre and a fibre volume fraction of 1.5 % demonstrated the best performance during the three-point bending test, achieving a fivefold increase in the maximum bending stress compared to pure silica aerogel samples with up to 33 kPa.

1. Introduction

Silica aerogels are known as a light and highly insulating material due to their low thermal conductivity with a minimum of 0.005 W/(m*K). The density is typically within the range of 0.003 and 0.35 g/cm³. The porosity of aerogels reaches up to 99,8 % while the pore size typically varies between 5 nm and 100 nm. As a result of their open-pored structure, silica aerogels show a specific surface area around 600 – 1000 m²/g. The white or milky materials feature a low dielectric constant $k = 1,0 - 2,0$ and the acoustic velocity within silica aerogels is $c = 100$ m/s (Soleimani Dorcheh and Abbasi, 2008). Because of their properties, aerogels are used as insulation materials in buildings and windows, as filters and absorbers or in Cherenkov radiators (Cooper, 1989; Gesser and Goswami, 1989; Kajihara, 2013; Parmenter and Milstein, 1998).

Although aerogels are already used as insulation materials in some specialty applications, the aerogels feature inadequate mechanical properties for a more widespread application. Fragility and low strength are current issues on the way for application in widespread building insulation. To improve these deficits, studies have been conducted on fibre reinforced aerogels with different fibrous materials since the 1990s (Ślosarczyk, 2017). Fibre reinforced composites are made of fibres and a matrix material in order to improve the mechanical properties (Henning and Moeller, 2011). Chopped inorganic fibres such as ceramic and glass fibres or chopped organic fibres such as carbon and polymer fibres were used to reinforce aerogels (Ślosarczyk, 2017). The bond between the reinforcement fibres and aerogels is generally based on adhesion, rarely on chemical bonding (Li et al., 2016).

Due to the low-viscosity of the sol during the aerogel production, reinforcement fibres can quickly deposit as sediment when added to the sol. Several approaches for special embedment methods of fibres to avoid sedimentation have been suggested in literature. One approach is the two-step catalysis in which the viscosity is controlled until a point is reached where sedimentation is prevented. After the addition of the reinforcement fibres the gelation is completed (Maleki et al., 2014; Ślosarczyk, 2017). In a further approach the short fibres are texturized by the means of a cutting mill. A three dimensional structure of entangled fibres is thereby formed before the fibres are added to the sol (Markevicius et al., 2017). Previous studies have shown that fibrous reinforcement has an impact on the shrinkage, the mechanical properties and the thermal conductivity

of aerogels depending on fibre volume fraction and the length of the fibres. Jaxel et al. (2017) have shown that the shrinkage of 17 % can be reduced to 5 % - 6 % Mechanical properties like flexural strength, Young's modulus, fracture strain and compression modulus were increased by the addition of fibrous reinforcement in further studies on fibre reinforced aerogels (Jaxel et al., 2017; Li et al., 2016; Shi et al., 2013; UI Haq et al., 2017; Yang et al., 2011; Zhihua et al., 2008). Moreover, fibres are holding the aerogel matrix together so that specimen would not break in two pieces during three-point bending test (Jaxel et al., 2017). In contrast to pure aerogels, the thermal conductivity of fibre reinforced aerogels is higher according to Li et al. (2016). Nevertheless, the fibre material has an effect on the thermal conductivity (Jaxel et al., 2017; Maleki et al., 2014).

Basalt fibre reinforced silica aerogels have not been produced or tested with regards to their mechanical properties to date. Basalt fibres are made of naturally occurring basaltic rocks and are non-toxic. Similar to silica aerogels, the fundamental structure of basalt fibres is made up of SiO_2 (> 50 %) as the network former. This makes basalt fibres particularly interesting for insulation products based on silica aerogels.

2. Experimental Procedure

Basalt fibres of 3.2 mm and 12.7 mm length with a diameter of 13 μm , produced by Kamenny Vek (Russia) and distributed by BASALTEX[®] NV (Belgium) were used as the fibrous reinforcement. The aerogel matrix was produced by a sol-gel process similarly to Shao et al. (2017). The precursor methyltriethoxysilane (MTES) has a chemical purity of 98 % and the solvent, in this case ethanol, has a purity of ≥ 99.8 %. Both chemical substances were used as a catalyst and they were purchased from Merck KGaA (Germany). Ammonia with a concentration of 30 – 33 mol% was used as a catalyst. Five composite samples were produced with different fibre types and fibre volume contents (Table 1).

Table 1: Specimen specification

Specimen test series number	S1	S2	S3	S4	S5
fibre length [mm]	3.2	3.2	12.7	12.7	-
fibre volume content [%]	0.75	1.5	0.75	1.5	0

Ethanol, deionized water and MTES were mixed with a volume ratio of 1:1.1:0.5. Afterwards, the solution was stirred in a closed container at 150 rpm for 72 h at room temperature for hydrolyzation. Subsequently, one drop of ammonia per 10 ml solution was added as catalyst and the sol was stirred again for a further 5 minutes. Finally, the sol was poured into 80 mm x 20 mm x 10 mm aluminium moulds containing basalt fibres. The chopped basalt fibres were expanded following the basic concept of Jaxel et al. (2017). The fibres were inserted in to a short pipe and texturized by turbulent air flow. The texturized fibres were inserted into the sol. The basalt fibre reinforced aerogel aged for 48 h in an oven at 55 °C. While aging, the composites were covered with ethanol. The ethanol was exchanged after a period of 24 h. The specimens aged and dried within the mould. Finally, the specimens were dried for 24 h in an oven at 80 °C. With this procedure eight specimens were produced per series.

The dimensions and weight of each specimen were registered. The outer dimensions were obtained by the means of a vernier calliper (Hoffmann Group, accuracy ± 0.05 mm) and the weight was measured with an analytic balance (Mettler Toledo XPE205, accuracy ± 0.01 mg). X-Ray computed tomography was used to analyse the internal microstructure of the composite. Two specimens per test series were recorded by a procon X-Ray CT-Alpha with a resolution of 25 μm . A three-point bending test on the basis of DIN EN ISO 14125 was carried out. A velocity of $v = 1$ mm/s with a 10 N load cell was applied. The tests were terminated when 50 % of F_{max} was reached. An outer span of $L = 64$ mm was selected.

3. Results and Discussion

Shrinkage

Based on the recorded dimensions, the volume was calculated for the specimens. Subsequently, the shrinkage is calculated as the reduction in volume before and after drying. As shown in Figure 1a, the introduction of basaltic reinforcement fibres significantly lowers the volume shrinkage of the composite occurring during the drying process. The fibre network acts as a supporting skeleton when drying and keeps the aerogel in its original shape. In comparison to previous experiments, such as those performed by Jaxel et al. (2017) where a maximum shrinkage of 17 % was recorded, the shrinkage of unreinforced aerogels in these experiments is higher. However, a different synthesis based on tetraethoxysilane was employed by Jaxel et al. (2017). The shrinkage drastically decreases with increasing fibre volume contents. Increasing the fibre volume

fraction to from 0.75 % to 1.5 % reduced the average shrinkage by over 50 %. No significant impact of the fibre length on the shrinkage could be observed. This trend is similar to that observed by Jaxel et al. (2017).

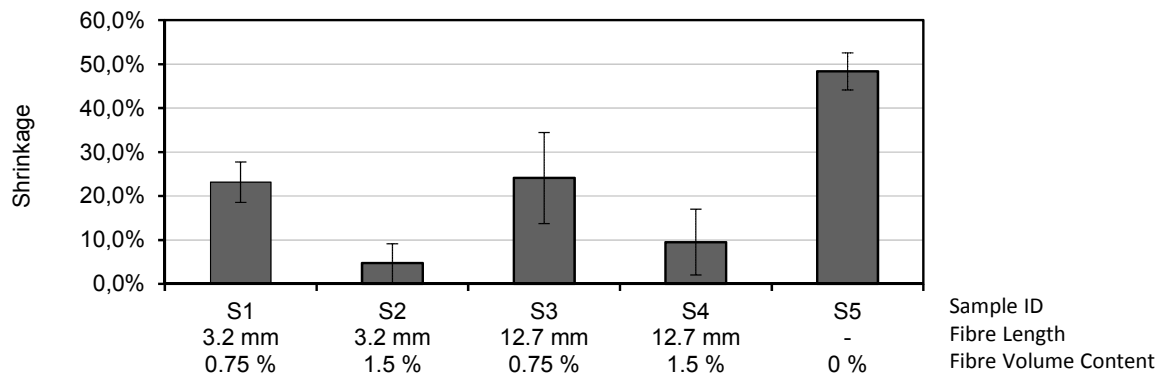


Figure 1: Volumetric shrinkage of aerogel during ambient pressure drying.

Fibre distribution and internal structure

In order to understand and evaluate the mechanical behaviour of fibre reinforced aerogels, it is necessary to examine the distribution of fibres within the matrix. In contrast to 3.2 mm fibres, longer 12.7 mm fibres show a tendency to form layers. Sedimentation is observed for low fibre volume fractions (Figure 2c). Sedimentation of the fibrous reinforcement is greatly reduced for fibre volume content of 1.5 %. An incompletely textured chopped basalt fibre roving is indicated by (I). A rolled structure that can be recognised in the sample shown in Figure 2 d), which is a result of the embedding of the reinforcement fibres. The fibres are not distributed fully homogenous within the composites shown in Figure 2. The computed tomography image also indicates the enclosure of air. For short fibres, small air pockets (II) can be identified in Figure 2, whereas bigger pockets appear in specimen with 12.7 mm fibres (V). Furthermore, sub-surface cracks are visible inside aerogels reinforced with long fibres (III), (IV). The crack paths indicate the main function of the reinforcing fibres, namely the redirection of cracks and the prevention of crack expansion.

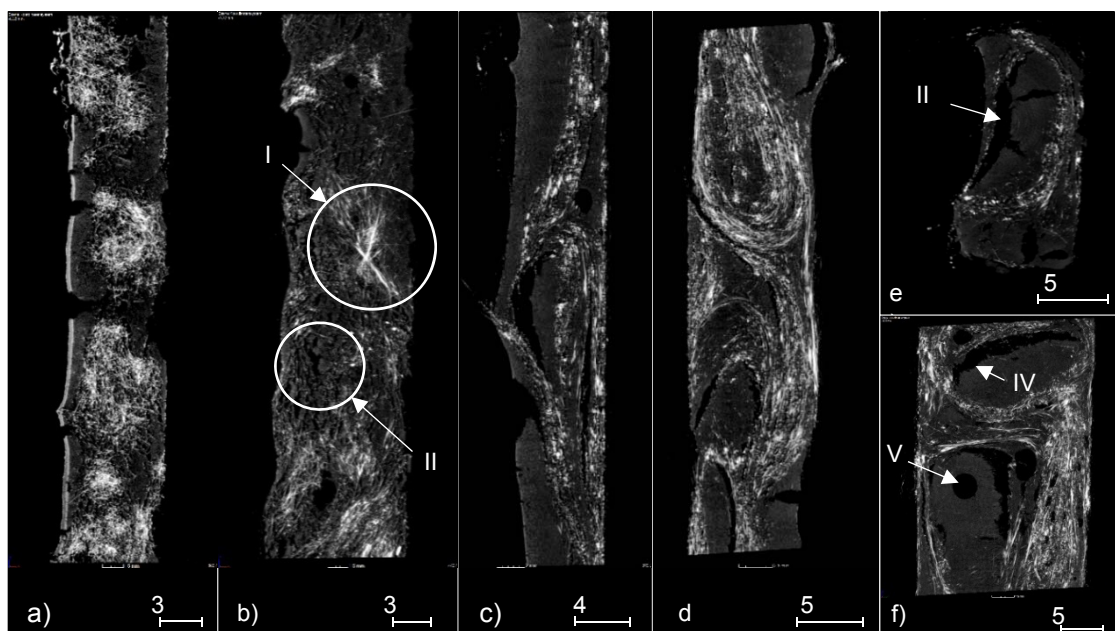


Figure 2: Computed tomography images: a): fibre clustering; b): homogeneous distribution; c), e): fibre sedimentation; d), f): fibre rolling

Mechanical Properties

The reinforced aerogels show greatly improved mechanical strength. While three out of eight pure aerogel specimens failed due to the mechanical load during the de-moulding process, all 32 reinforced specimens could be extracted from the mould as monolithic samples. Figure 3 illustrates the flexible strength determined during the three-point bending test of the different samples. The reinforced samples show a greatly improved mechanical strength. Higher mechanical strengths were achieved by the longer reinforcement fibres of 12.7 mm length. While the average strength of samples from the S4 series with 12.7 mm long fibres and 1.5 % fibre volume content showed an average flexural strength of 33 kPa, the samples from the S5 series without any reinforcement only showed a flexural strength of 6 kPa. Samples from the S2 series with 3.2mm long reinforcement fibres and a fibre volume content of 1.5 % reached an average bending strength of 23 kPa. Large standard deviations indicate the variation in fibre distribution as well as voids within the composites. Besides the flexible strength, the stress-bending-curve obtained by the three-point bending test provides additional information on the mechanical behaviour of the specimens.

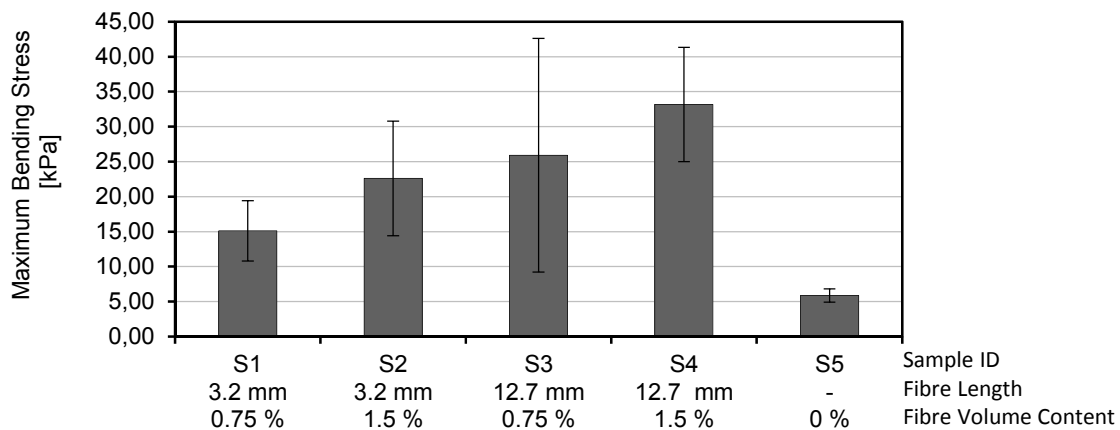
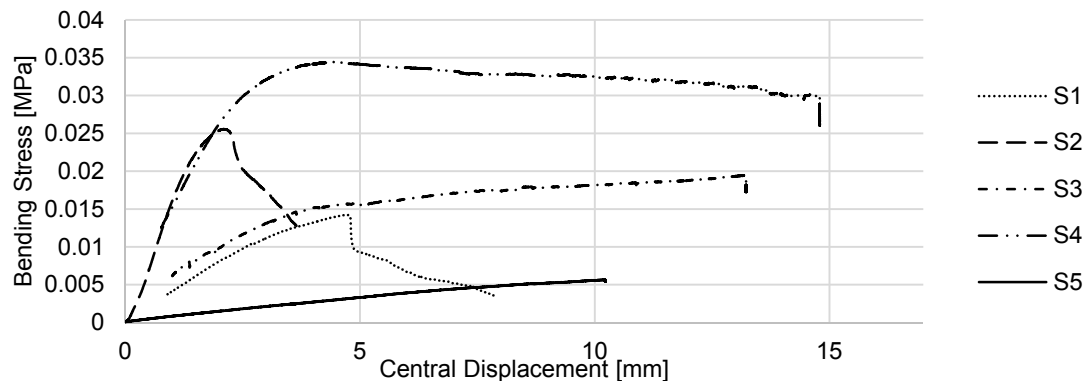


Figure 3: Maximum bending stress of the samples S1 – S5 under three point bending



In Figure 4, an indicative sample stress-strain-curve for one specimen per series is plotted. An almost linear stress-strain path can be observed for the unreinforced aerogel sample S5. Failure occurs straight after reaching a peak stress without any pre-failure or plateau. The samples reinforced with short fibres of 3.2 mm length show a distinctive peak strength with subsequent rapid failure. Upon failure of the matrix, the reinforcement fibres are not long enough to bridge the point of fracture in the composite. This leads to a rapid decrease in strength. The samples reinforced with 12.7 mm long fibres from the series S3 and S4 however do not show the same rapid loss of strength after reaching their peak strength. The longer reinforcement fibres are able to bridge the point of fracture in the composite matrix and thereby retain the bending strength at least partially. The strength reduces as the fibres are pulled out from the matrix with increasing loads. Sample S3 shows a distinct region of plastic deformation after reaching an initial failure point at 4mm central displacement. Furthermore, it should be noted that young's modulus increases with increasing basalt fibre volume contents.

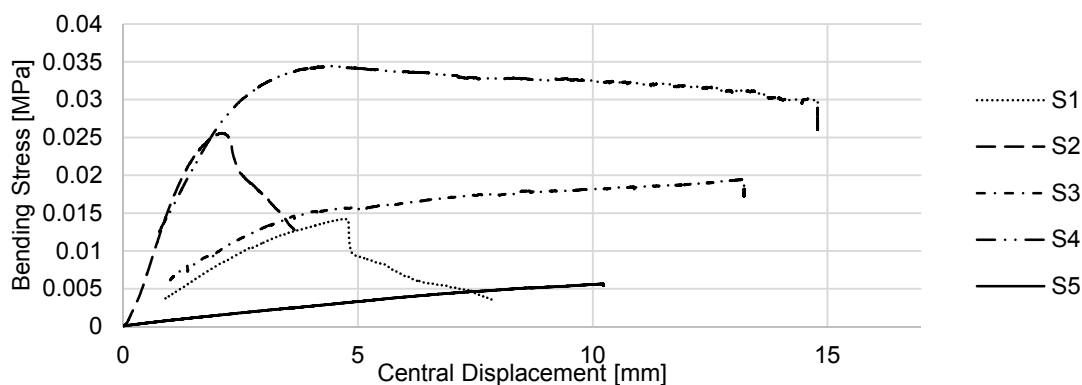


Figure 4: Three-point bending curve for selected specimens of each series

Crack propagation

The phenomenon of reinforcement fibres bridging cracks within the matrix as mentioned above is also visible in Figure 5. As shown in Figure 5a, composites reinforced with 3.2 mm fibres tend to break into two parts whereas none of the specimens with 12.7 mm fibres show this behaviour. While the crack in specimens of series S1 (Figure 5a) are relatively straight, a higher fibre fraction deflects the cracks. Nevertheless, the crack remains within a vertical plane. The crack deflection in series S3 and S4 forces the crack to leave this vertical plane as it can be seen in Figure 5c. Figure 5d shows how the crack is completely stopped. Failure occurs without complete separation of the sample.

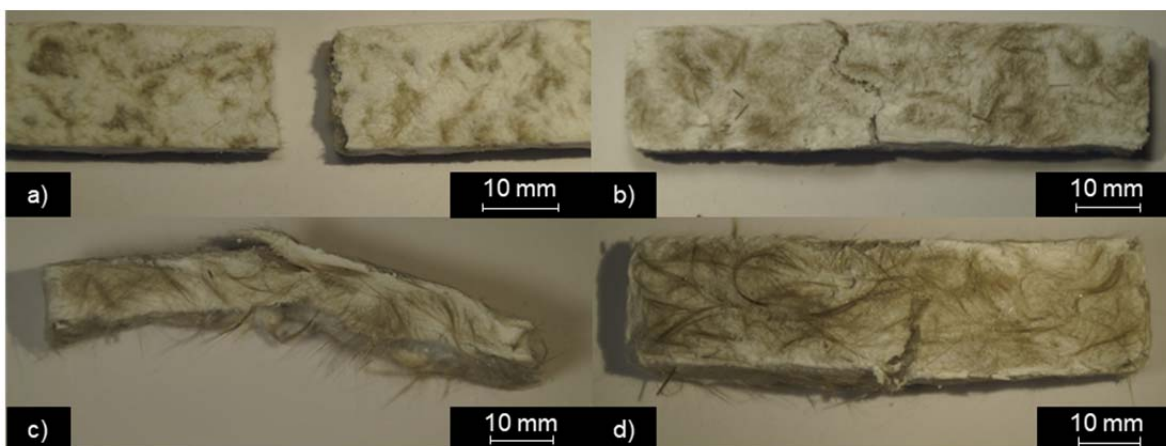


Figure 5: Failure type after three-point bending test, a) S1; b) S2; c) S3; d) S4

4. Conclusion

Basalt fibre reinforced aerogel composites have been produced for the first time. The best result regarding the mechanical properties was achieved for specimens with fibres of 12.7 mm length and 1.5 % fibre volume content. The maximum bending stress increased over fivefold for these samples in comparison to the reference samples without any fibrous reinforcement to 33 kPa. Furthermore the shrinkage of the samples decreased to a fifth of the reference specimens to 4.7 %. This optimization of the mechanical properties of basalt fibre reinforced aerogels is a first step to enable the use of such composites as conventional insulation panels. However, further investigations need to be conducted in order to determine the impacts of different methods for fibre embedment. Furthermore, other properties such as the thermal conductivity need to be analysed for different combinations of basalt fibres and aerogels.

Acknowledgments

This work is part of the project “AeroBasalt” financed by the Federal Ministry of Education and Research Germany within the framework of “KMUinnovativ Materialforschung”. Grant number: 13XP5039B.

References

- Cooper, D.W., 1989, Theoretical study of a new material for filters: Aerogels, *Particulate Science and Technology* 7 (4), 371–380.
- Gesser, H.D., Goswami, P.C., 1989, Aerogels and related porous materials, *Chemical Reviews* 89 (4), 765–788.
- Henning, F., Moeller, E., 2011, *Handbuch Leichtbau: Methoden, Werkstoffe, Fertigung*, Hanser, Munich, Germany.
- International Standards Organisation. 2011, DIN EN ISO 14125 : Fibre-reinforced plastic composites - Determination of flexural properties. Germany
- Jaxel, J., Markevicius, G., Rigacci, A., Budtova, T., 2017, Thermal superinsulating silica aerogels reinforced with short man-made cellulose fibers, *Composites Part A: Applied Science and Manufacturing* 103, 113–121.
- Kajihara, K., 2013, Recent advances in sol–gel synthesis of monolithic silica and silica-based glasses, *Journal of Asian Ceramic Societies* 1 (2), 121–133.
- Li, Z., Cheng, X., He, S., Shi, X., Gong, L., Zhang, H., 2016, Aramid fibers reinforced silica aerogel composites with low thermal conductivity and improved mechanical performance, *Composites Part A: Applied Science and Manufacturing* 84, 316–325.
- Maleki, H., Durães, L., Portugal, A., 2014, An overview on silica aerogels synthesis and different mechanical reinforcing strategies, *Journal of Non-Crystalline Solids* 385, 55–74.
- Markevicius, G., Ladj, R., Niemeyer, P., Budtova, T., Rigacci, A., 2017, Ambient-dried thermal superinsulating monolithic silica-based aerogels with short cellulosic fibers, *Journal of Materials Science* 52 (4), 2210–2221.
- Parmenter, K.E., Milstein, F., 1998, Mechanical properties of silica aerogels, *Journal of Non-Crystalline Solids* 223 (3), 179–189.
- Shao, Z., He, X., Cheng, X. and Zhang, Y. (2017). A simple facile preparation of methyltriethoxysilane based flexible silica aerogel monoliths. *Materials Letters*, Volume 204, 93-96,
- Shi, D., Sun, Y., Feng, J., Yang, X., Han, S., Mi, C., Jiang, Y., Qi, H., 2013, Experimental investigation on high temperature anisotropic compression properties of ceramic-fiber-reinforced SiO₂ aerogel, *Materials Science and Engineering: A* 585, 25–31.
- Ślosarczyk, A., 2017, Recent Advances in Research on the Synthetic Fiber Based Silica Aerogel Nanocomposites, *Nanomaterials* 7 (2).
- Soleimani Dorcheh, A., Abbasi, M.H., 2008, Silica aerogel; synthesis, properties and characterization, *Journal of Materials Processing Technology* 199 (1), 10–26.
- UI Haq, E., Zaidi, S.F.A., Zubair, M., Abdul Karim, M.R., Padmanabhan, S.K., Licciulli, A., 2017, Hydrophobic silica aerogel glass-fibre composite with higher strength and thermal insulation based on methyltrimethoxysilane (MTMS) precursor, *Energy and Buildings* 151, 494–500.
- Yang, X., Sun, Y., Shi, D., Liu, J., 2011, Experimental investigation on mechanical properties of a fiber-reinforced silica aerogel composite, *Materials Science and Engineering: A* 528 (13), 4830–4836.
- Zhihua, Z., Jun, S., Xingyuan, N., Yang, L., Jichao, W., Guangming, W., Bin, Z., Guoqing, W., Peiqing, W., Qingfeng, W., Xixian, N., 2008, Mechanical reinforcement of silica aerogel insulation with ceramic fibers, 371–374.